HHS Public Access

Author manuscript

Circ Arrhythm Electrophysiol. Author manuscript; available in PMC 2024 February 01.

Published in final edited form as:

Circ Arrhythm Electrophysiol. 2023 February ; 16(2): e010858. doi:10.1161/CIRCEP.122.010858.

Reduction in Junctophilin 2 Expression in Cardiac Nodal Tissue Results in Intracellular Calcium-driven Increase in Nodal Cell Automaticity

Andrew P. Landstrom, MD, PhD[1,2], **Qixin Yang, MD**[1,3], **Bo Sun, PhD**[1], **Robin M. Perelli, MS**[2], **Minu-Tshyeto Bidzimou, BA**[2], **Zhushan Zhang, MD, PhD**[2], **Yuriana Aguilar-Sanchez, PhD**[4], **Katherina M. Alsina, PhD**[4], **Shuyi Cao, MS**[5], **Julia O. Reynolds, BS**[5], **Tarah A. Word, PhD**[5], **Niels M.R. van der Sangen, MD**[5], **Quinn Wells, MD, PharmD, MSC**[6], **Prince J. Kannankeril, MD, MSCI**[7], **Andreas Ludwig, MD, PhD**[8], **Jeffrey J. Kim, MD**[9], **Xander H.T. Wehrens, MD, PhD**[5,9,10]

[1]Dept of Pediatrics, Division of Cardiology, Duke Univ School of Medicine, Durham, NC

[2]Dept of Cell Biology, Duke Univ School of Medicine, Durham, NC

[3]Dept of Cardiology, The First Affiliated Hospital, College of Medicine, Zhejiang Univ, Hangzhou, China

[4]Integrative Molecular & Biomedical Sciences Program, Baylor College of Medicine, Houston, TX

[5]Dept of Molecular Physiology & Biophysics, Baylor College of Medicine, Houston, TX

[6]Depts of Medicine, Pharmacology, and Biomedical Informatics, Vanderbilt Univ School of Medicine, Nashville, TN

[7]Center for Pediatric Precision Medicine, Dept of Pediatrics, Vanderbilt Univ School of Medicine, Nashville, TN

[8]Institut für Experimentelle und Klinische Pharmakologie und Toxikologie, Friedrich-Alexander-Universität Erlangen-Nürnberg, Erlangen, Germany

[9]Dept of Pediatrics, Section of Cardiology, Baylor College of Medicine, Houston, TX

[10]Depts of Neuroscience & Center for Space Medicine and the Cardiovascular Research Institute, Baylor College of Medicine, Houston, TX

Abstract

Background: Spontaneously depolarizing nodal cells comprise the pacemaker of the heart. Intracellular calcium (Ca^{2+}) plays a critical role in mediating nodal cell automaticity and understanding this so-called "Ca^{2+} clock" is critical to understanding nodal arrhythmias. We previously demonstrated a role for junctophilin-2 (Jph2) in regulating Ca^{2+}-signaling through

Correspondence: Andrew P. Landstrom, MD, PhD, Duke University Medical Center, Box 2652, Durham, NC 27710, Tel: 919-684-3028, andrew.landstrom@duke.edu; Xander H.T. Wehrens, MD, PhD, Baylor College of Medicine, One Baylor Plaza, BCM335, Houston, TX 77030, Tel: 713-798-4261, wehrens@bcm.edu.

Disclosures: X.H.T.W. is a co-founder and Scientific Advisory Board member of Elex Biotech, a drug development company focused on novel compounds for the cardiac arrhythmia disorders and heart failure. All other authors have no disclosures.

inhibition of ryanodine receptor 2 (RyR2) Ca^{2+} leak in cardiac myocytes; however, its role in pacemaker function and nodal arrhythmias remains unknown. We sought to determine whether nodal Jph2 expression silencing causes increased sinoatrial and atrioventricular nodal cell automaticity due to aberrant RyR2 Ca^{2+} leak.

Methods: A tamoxifen-inducible, nodal tissue-specific, knockdown mouse of Jph2 was achieved using a Cre recombinase-triggered short RNA hairpin directed against Jph2 (Hcn4:shJph2*). In vivo* cardiac rhythm was monitored by surface ECG, implantable cardiac telemetry, and intracardiac electrophysiology (EP) studies. Intracellular Ca^{2+} imaging was performed using confocal-based line scans of isolated nodal cells loaded with fluorescent Ca^{2+} reporter Cal-520. Whole cell patch clamp was conducted on isolated nodal cells to determine action potential kinetics and Ncx1 function.

Results: Hcn4:shJph2 mice demonstrated a 40% reduction in nodal Jph2 expression, resting sinus tachycardia and impaired heart rate response to pharmacologic stress. *In vivo* intracardiac EP studies and *ex vivo* optical mapping demonstrated accelerated junctional rhythm originating from the atrioventricular node. Hcn4:shJph2 nodal cells demonstrated increased and irregular Ca^{2+} transient generation with increased Ca^{2+} spark frequency and Ca^{2+} leak from the sarcoplasmic reticulum. This was associated with increased nodal cell AP firing rate, faster diastolic repolarization rate, and reduced Ncx1 activity during repolarized states compared to control. Phenome-wide association studies (PheWAS) of the *JPH2* locus identified an association with sinoatrial nodal disease and atrioventricular nodal block.

Conclusions: Nodal-specific Jph2 knockdown causes increased nodal automaticity through increased Ca^{2+} leak from intracellular stores. Dysregulated intracellular Ca^{2+} underlies nodal arrhythmogenesis in this mouse model.

Keywords

Automaticity; calcium; junctophilin 2; Jph2; sinoatrial node; pacemaker

Introduction

The nodal and conduction system of the heart play a critical role in the generation and propagation of the electrical depolarization which initiates cardiac myocyte contraction[1]. In the normal heart, the sinoatrial (SA) node automatically depolarizes and triggers a wave of electrical depolarization that causes atrial contraction[2, 3]. Depolarization is then delayed at the atrioventricular (AV) node, allowing for contraction of the atria and ventricular filling, before being propagated down ventricular bundle branches and the Purkinje fiber network. This coordinated depolarization of the ventricles allows for efficient contraction that ejects blood into pulmonary and systemic circulation. A broad class of arrhythmias, nodal arrhythmias are characterized by impaired automaticity or function of the SA and AV nodes, and are associated with fatigue, syncope, and even death[4]. Arrhythmias impacting the nodal or electrical conduction system of the heart are common and impact up to ~1% of the population, yet there are limited pharmacologic therapies to treat these arrhythmias[5]. This reflects the need for additional understanding of the molecular mechanisms of nodal cell automaticity.

Classically, spontaneous action potential generation of pacemaker cells has been viewed as a coordinated event among membrane-limited ion channels creating a so-called “membrane voltage clock”[4]. Recent evidence from multiple investigators suggests that there is an intracellular “calcium (Ca^{2+}) clock” which plays a critical role in impulse generation through rhythmic, spontaneous release of Ca^{2+} from the intracellular sarcoplasmic reticulum (SR) store via RyR2[6]. Indeed, nodal cell Ca^{2+} signaling may be a potential molecular target for pharmacologic manipulation as altered Ca^{2+} signaling has been associated with both physiological nodal cell depolarization and dysfunction[7, 8]. *Jph2*-encoded junctophilin-2 (Jph2) is a structural protein that plays a critical role in Ca^{2+} regulation within the contractile myocytes of the heart[9]. We have previously shown that Jph2 expression knockdown in cardiomyocytes causes increased Ca^{2+} leak from intracellular stores (i.e. the SR) resulting in heart failure through dysregulation of the intracellular Ca^{2+} release channel RyR2[10-12]. Follow-up studies have shown that Jph2 serves as a molecular regulator of intracellular Ca^{2+} and that a defective Jph2-RyR2 interaction may be targeted by small molecules to prevent pathologic Ca^{2+} leak[13]. This makes Jph2 a unique molecule to dissect the underlying role of Ca^{2+} dysregulation in nodal disease and a possible target for therapeutic intervention.

To this end, we report a conditional, nodal-specific Jph2 knockdown which causes increase nodal cell automaticity. Further, we found that this increase in automaticity is associated with increased SR store Ca^{2+} leak. Finally, phenome-wide association studies (PheWAS) of the *JPH2* locus identified an association with sinoatrial nodal disease and atrioventricular nodal block. These findings suggest a possible role for Jph2 deficit-induced aberrant Ca^{2+} homeostasis and signaling in the development of nodal arrhythmias.

Methods

The data the support the findings of this study are available from the corresponding author upon reasonable request

Transgenic Mice

All mice were treated in accordance with the Baylor College of Medicine and the Duke University School of Medicine Institutional Animal Care and Use Committees, respectively, and reflected proposed guidelines for rigor and reproducibility in preclinical animal studies[14]. A nodal-specific, conditional Jph2 knockdown transgenic line was achieved by crossing two lines to create a double transgenic line. The nodal-specific Hcn4-KiT Cre mouse was previously described[15]. Briefly, this line expresses tamoxifen-inducible $CreER^{T2}$ inserted into the pacemaker channel *Hcn4* locus (Hcn4). Previous studies have demonstrated robust expression of Cre selectively to nodal tissue without modulation of cardiac rhythm, basal heart rate (HR), or HR variability[15]. This line was crossed with a mouse line expressing a Jph2 shRNA[12]. This shJph2 was placed under the transcriptional control of a high-expression U6 promoter inhibited by a neomycin cassette with flanking *loxP* sites. Presence of Cre-recombinase floxed out this inhibitory cassette allowing for inducible shJph2 expression. This created the Hcn4:shJph2 double transgenic line which was the experimental group (referred to as shJph2). Mice were injected IP with tamoxifen at approximately 3 months of age as described[12], and all experiments were

conducted at 4-6 months of age. Littermate control mice carrying the Hcn4 Cre (Hcn4:WT) following tamoxifen injection were used as the controls for all studies. Cre-expression was confirmed utilizing the mTmG double-fluorescent Cre reporter mouse that expresses membrane-targeted tdTomato (mT) prior to Cre-recombination, and membrane-targeted GFP (mG) post Cre-excision[16]. All transgenic mice were on a C57BL/6J background. Due to sex-specific effects of tamoxifen on female mice physiology, including the cardiovascular system, male mice were utilized[17, 18]. Mice were euthanized under isoflurane anesthesia using cervical dislocation. Additional details, including additional methods, are included in the Supplemental Materials.

Results

Hcn4:shJph2 mice demonstrate nodal-specific Jph2 knockdown

To determine whether loss of Jph2 expression results in increased nodal automaticity, a double transgenic mouse line Hcn4:shJph2 was created (Figure 1A). Following tamoxifen induction (Figure 1B), robust Cre-expression was confirmed by crossing the Hcn4:shJph2 mice with the mTmG reporter line which shifts changes RFP expression into GFP in the presence of Cre. We identified robust GFP expression in the SA node, AV node, and His-Purkinje/bundle branches, in cardiac sections from Hcn4:mTmG mice (Sup Figure I). Hcn4:shJph2 mice demonstrated normal growth and survival both pre- and post-induction with no loss of cardiac systolic function by transthoracic echocardiogram. Further, Hcn4:shJph2 mice demonstrated a 42.5±0.4% reduction in Jph2 mRNA expression by qPCR in excised AV nodal tissue compared to control (P<0.0001, Figure 1C). Further, immunofluorescence of Jph2 in Hcn4-expressing cells identified by histology of Hcn4:shJph2:mTmG mouse hearts identified a 33±2.5% reduction in Jph2 fluorescent intensity compared to control Hcn4:WT:mTmG control mice in both the SA and AV node (P<0.0001, Sup Figure II). Hcn4 mRNA levels were not altered in Hcn4:shJph2 SA nodal tissue compared to Hcn4:WT controls (Figure 1D). Further, there was no change in mRNA expression of Ryr2 and the cardiac sodium-calcium exchanger (Ncx1) in knockdown mice compared to controls (Figure 1E and 1F). To exclude the possibility that any heart rate or rhythm abnormality was secondary to elevated plasma catecholamine levels, serum ELISA was performed which demonstrated no alteration to circulating epinephrine and norepinephrine levels in Hcn4:shJph2 mice compared to controls (Figure 1G).

Hcn4:shJph2 mice demonstrate increased heart rates with blunted adrenergic modulation

To evaluate the impact of Jph2 knockdown on cardiac conduction and rhythm, Hcn4:shJph2 mice were first evaluated by surface ECG and ambulatory ECG telemetry. Hcn4:shJph2 mice exhibited a mildly increased sinus node recovery time (SNRT:123±3 ms) and QRS duration (8.7±0.3 ms) compared to controls (SNRT:111±1 ms, QRS:7.6±0.2 ms, respectively, P=0.02) consistent with intraventricular conduction delay. There was no change in PR, QT, and QTc intervals (Figure 2A and 2B, Sup Table I). Ambulatory ECG telemetry demonstrated no change in HR over a 24-hour period in Hcn4:shJph2 mice compared to control prior to tamoxifen-induction. However, following Jph2 knockdown, Hcn4:shJph2 mice demonstrated an increase in HR of 13.9% throughout the day from a mean of 583.6±14.4 bpm compared to controls of 512.1±13.6 bpm (P=0.003). This HR increase

persisted throughout the sleep-wake cycle of the mice (Figure 2C and 2D). Taken together, these findings suggest increased SA nodal automaticity and intraventricular conduction delay without evidence of AV nodal block.

To test whether HR responsiveness to pharmacologic modulation was altered, telemetry-implanted mice were challenged with IP drug injections. Beta adrenergic stimulation (epinephrine, isoproterenol) caused increased HR in both Hcn4:shJph2 mice and controls. However, maximal HR achieved was blunted with Jph2 knockdown (618.6±10.5 bpm in Hcn4:shJph2 mice following epi, compared to 696.7±8.7 bpm in control, P=0.005; 741.1±0.5 bpm in Hcn4:shJph2 vs 770.8±8.9 bpm in control following iso, P=0.0002). Similarly, the HR-slowing effect of beta blockade (propranolol, 460.0±20.9 bpm in Hcn4:shJph2 vs 404.3±11.7 in control, P=0.02) and cardiac Na^+/K^+-ATPase blockade (digoxin, 413.7±15.4 bpm in Hcn4:shJph2 vs 320.5±32.6 bpm in control, P=0.03) was blunted compared to controls. This blunted modulation of HR was not seen with muscarinic receptor agonists (carbachol) and antagonists (atropine) (P=NS, respectively; Figure 2E). Hcn4:shJph2 mice demonstrated no spontaneous atrial ectopy or arrhythmias, ventricular ectopy or arrhythmias, or atrioventricular block on 24-hour telemetry. Taken together, these findings were consistent with increased automaticity of SA node with evidence for impaired responsiveness to beta-adrenergic modulation.

Hcn4:shJph2 mouse hearts demonstrate accelerated junctional rhythm *in vivo* and *ex vivo*

To evaluate intracardiac rhythm and arrhythmia inducibility, Hcn4:shJph2 mice were subjected to *in vivo* intracardiac EP studies. While control mice demonstrated sinus rhythm with clear electrical association between the atria and ventricles, knockdown mice demonstrated a high incidence of atrioventricular dissociation with ventricular depolarization occurring independently of the sinus node and faster than atrial depolarization without a change in QRS or ventricular depolarization morphology (Figure 3A). This was consistent with an accelerated junctional rhythm (AJR) driven by increased automaticity of the AV node. Spontaneous AJR was observed in 56% of Hcn4:shJph2 mice at baseline and was not observed in any of the control mice (P=0.004, Figure 3B). IP isoproterenol injection in knockdown mice triggered AJR in 78% of mice while no control mice demonstrated the arrhythmia (P<0.001, Figure 3C). Complete intracardiac EP study findings are summarized in the Sup Table I.

To confirm that this finding was intrinsic to the heart, and not secondary to non-cardiac influences such as sympathetic or parasympathetic innervation, hearts from Hcn4:shJph2 mice were Langendorff-perfused and *ex vivo* optical mapping was performed. Consistent with intracardiac EP studies, optical imaging of the heart's electrical depolarization demonstrated spontaneous AJR manifest as ventricular depolarization without preceding right atrial depolarization (Figure 3D). This was confirmed by superimposition of myocardial voltage maps with visualization of the AV node at the crest of the intraventricular septum, which demonstrated AV node depolarization preceding ventricular depolarization without atrial depolarization (Sup Figure III). Taken together, these findings suggest that Hcn4:shJph2 mice have a predisposition to increased AV nodal automaticity which manifests as AJR.

Epicardial *ex vivo* rhythm monitoring of Hcn4:shJph2 hearts demonstrate junctional rhythm and inducible junctional tachycardia

To conclusively define the *ex vivo* cardiac rhythm, customized epicardial electrodes were placed directly on excised Hcn4:shJph2 heart atria and ventricles during retroaortic perfusion. Consistent with previous findings, 44% of Hcn4:shJph2 *ex vivo* hearts demonstrated AJR at baseline while none of the control hearts demonstrated AJR (P=0.04). Isoproterenol bolus into the cardiac perfusate induced a rapid onset junctional ectopic tachycardia (JET) with a rhythm significantly faster than AJR in 89% of knockdown mice while control mice demonstrated sinus rhythm (P<0.001, Figure 4A-F). To test whether antagonists of RyR2 opening terminated JET, we first treated mice with flecainide, which has been previously shown to reduce Ca^{2+} leak from RyR2 in cardiac myocytes without direct binding to RyR2[19]. Flecainide bolus into the perfusate did not terminate JET and frequently induced ventricular arrhythmias. In contrast, a similar perfusate bolus of a specific small molecule RyR2 inhibitor, EL20[20], abruptly terminated JET in 88% of knockdown mice with JET (P=0.01). In some cases, EL20 terminated successive episodes of isoproterenol-triggered JET in the same mouse with an overall conversion rate of 76% for all JET events (P=0.01, Figure 4G). These findings suggest that quickly administered beta agonists are able to trigger a rapid tachycardia from the AV node, consistent with JET, which can be converted to sinus rhythm with inhibition of RyR2.

Jph2 knockdown causes increased frequency and decreased amplitude of calcium transients in SA nodal calls

To determine whether intracellular Ca^{2+} signaling was associated with increased cell automaticity, we isolated SA nodal cells from Hcn4:WT and Hcn4:shJph2 mice and conducted single-cell Ca^{2+} imaging with Cal-520 fluorescent Ca^{2+} dye. Isolated SA nodal cells demonstrated classic spindle- or spider-like morphology (Figure 5A) and spontaneous depolarization activity manifest as Ca^{2+} transients. Hcn4:shJph2 SA nodal cells demonstrated a faster frequency of spontaneous transients; however, the transients were irregular and frequently prematurely terminated without traveling the length of the cell (Figure 5B). Ca^{2+} transient kinetics were also measured (Figure 5C). Overall, Hcn4:shJph2 SA nodal cells demonstrated an approximately 5-fold increase in transient frequency (P<0.0001, Figure 5D) with a reduce transient amplitude (P<0.0001, Figure 5E) and transient time-to-peak (P=0.02, Figure 5F). Finally, time constant of transient decay (tau) was found to be reduced in Hcn4:shJph2 SA nodal cells compared to controls (P=0.002, Figure 5G). Overall, these findings demonstrate that Jph2 knockdown is associated with increased spontaneous Ca^{2+} transient frequency that are reduced in amplitude and reduction in SR Ca^{2+} release.

Jph2 knockdown causes increased store-calcium leak

In order to determine whether this increase in Ca^{2+} transient frequency was associated with increased Ca^{2+} leak from the SR Ca^{2+} store, we measured caffeine-triggered SR Ca^{2+} release and measured Ca^{2+} sparks. Hcn4:shJph2 SA nodal cells demonstrated a markedly reduced level of SR Ca^{2+} release compared to the control cells (Figure 6A-C). Calcium sparks were more frequent (P<0.0001) in Hcn4:shJph2 cells; however, demonstrated a

smaller amplitude (P=0.01), a trend toward smaller width (*P*=0.06), and duration (*P*=0.008) compared to controls (Figure 6D-H). As the result, the Jph2 knock down cells were calculated to have an approximately 20% higher amount of Ca^{2+} leak from SR compared to the control cells (*P*=0.001, Figure 6I). Taken together, the results suggest that increased Ca^{2+} leak from the SR leads to reduced levels of stored Ca^{2+} and is driven by increased RyR2 opening.

Jph2 knockdown is associated with increased rate of diastolic depolarization and increased cellular automaticity in SA nodal cells

To determine whether the increased transient frequency and store Ca^{2+} leak was associated with increased SA nodal cell automaticity, we recorded spontaneous action potentials (AP) in isolated single SA nodal cells. Compared to Hcn4:WT nodal cells, the firing rate of AP was significantly higher in Hcn4:shJph2 nodal cells (355±13 vs. 256±22 bpm, *P*=0.003, respectively) and the AP cycle length was markedly shorter (171±6 vs. 244±22 ms, *P*=0.005). The rate of the diastolic depolarization (DDR) also significantly higher in shJPH2 nodal cells (224±21 vs. 159±9 mV/s, *P*=0.04) and the duration of the diastolic depolarization (DI) was shorter in shJph2 cells (101±7 vs. 152±14, *P*=0.007, Figure 7A-F). Conversely, there were no significant changes in the maximum diastolic potential (MDP), the AP threshold potential (E_{-th}), the AP threshold (V_{-th}), AP amplitude (APA), AP duration, and dV/dt_{max} (Sup Figure IV). Moreover, some of the spontaneous membrane depolarizations were terminated early and failed to burst into action potentials (Sup Figure V), which was consistent with the observation that some Ca^{2+} transients were prematurely terminated without traveling the length of the nodal cell. Overall, these findings suggested increased automaticity in shJph2 SA nodal cells.

Jph2 knockdown causes reduced I_{NCX}

Given the increase in Ca^{2+} leak observed, and the established interplay between intracellular Ca^{2+} leak and Ncx function in ventricular myocytes[21], we next performed patch clamp analysis of I_{NCX}. We found that that I_{NCX} was reduced by approximately 50% in Hcn4:shJph2 nodal cells compared to control at −60 mV (*P*=0.03). Further, there was no significant difference in I_{NCX} at +80 mV (Figure 7G-I). Overall, this suggests that loss of Jph2 expression in nodal cells is associated with decreased Ncx function during resting membrane potentials.

JPH2 gene locus may be associated with clinical cases of nodal disease

To explore the possibility that the *JPH2* locus may be associated with nodal disease in humans, we next pursued PheWAS analysis of coding variants in *JPH2* using the BioVU platform. We identified 18 nominally significant associations with a P-value <0.01, including identified associations between variant rs3810510 (p.Ala396Thr) and several clinical diagnoses of SA and AV nodal disease. Among the top 13 phecodes were four cognate human diagnoses of phenotypes observed in our mouse experiments, including first degree AV block (OR 1.49, *P*=0.003), AV block (OR 1.26, *P*=0.004), SA node dysfunction (OR1.23, *P*=0.006) and Mobitz II AV block (OR 1.98, *P*=0.006). These results are summarized in Table 1 with a full list of the top PheWAS results summarized in

Sup Table II. These PheWAS findings suggest an important role *JPH2* in nodal disease in humans, although further studies are needed to establish this association.

Discussion

Store-calcium leak is associated with increased nodal automaticity

Action potential generation of the SA node is an automatic, yet highly regulated, event that is orchestrated by a complex interplay between the membrane voltage and Ca^{2+} clocks. Recent evidence from multiple investigators suggests that there is an intracellular Ca^{2+} clock which plays a critical role in impulse generation through rhythmic, spontaneous release of Ca^{2+} from intracellular SR stores via RyR2[6]. Here, we find that reduced Jph2 expression is associated with faster spontaneous nodal cell depolarizations and increased SR store Ca^{2+} leak *in vitro*, which manifests as sinus tachycardia and AV nodal tachycardia*, in vivo*. The identification of reduced I_{NCX} at negative membrane potentials in Hcn4:shJph2 mice, which is similar to controls a positive membrane potentials, suggests reduced Ca^{2+} efflux from the cell via Ncx during resting membrane states. This fits with a possible "Ca^{2+} overload" state that is driving increased cellular automaticity. In support of this, application of ryanodine to nodal cells, an inhibitor of RyR2 opening, causes slower heart rate[22]. In addition, build-up of SR store Ca^{2+} has been linked to recruitment of depolarizing currents which are a part of the membrane voltage clock, such as I_f created by Hcn4, $I_{L\text{-}Ca}$ from the L-type Ca^{2+} channel ($Ca_V1.2$), and $I_{T\text{-}Ca}$ from the T-type Ca^{2+} channels ($Ca_V3.1$ and 3.2). These currents serve to increase membrane potential spontaneously and coordinate to drive nodal depolarization[23]. In this way, it is believed that perturbed Ca^{2+}-signaling within the nodal cells, such as increased SR Ca^{2+} leak from RyR2, may result in loss of proper automaticity and nodal disease. We see evidence for this in both nodal cell Ca^{2+} transients and spontaneous APs which occur more rapidly yet can terminate before reaching either the full length of the cell or fully depolarize the cell, respectively. It is possible that this process can override the typical responsiveness of the nodal tissue to adrenergic and cholinergic regulation. Beta adrenergic stimulation of protein kinase A has been linked to increased nodal depolarization secondary to increased store Ca^{2+} release[24]. While we find that the heart rate responsiveness of Hcn4:shJph2 mice to chronotropic drugs, primarily adrenergic receptor agonists and antagonists, is blunted, additional studies are needed to confirm whether there is a difference in the impact of cholinergic versus adrenergic drugs on intracellular Ca^{2+} handling.

Jph2 negatively regulates RyR2-mediated calcium leak

While our study is the first to explore the role of Jph2 in nodal cells Jph2 has a well-established role in regulating Ca^{2+} release from the SR in ventricular myocardial cells, among other critical roles in the heart. Jph2 is a muscle-specific protein located in the junctional membrane complex (JMC) of the myocyte which plays a critical role in maintaining efficient intracellular Ca^{2+}-signaling for myocyte contraction as well as proper gating of RyR2[25]. As part of the JMC, Jph2 colocalizes with several sarcolemmal proteins and SR proteins that create the critical cellular ultrastructure needed for efficient Ca^{2+}-signaling[26]. Jph2 directly interacts with RyR2, and expression silencing results in increased RyR2 gating by lipid bilayer analysis and increased Ca^{2+} leak from the SR manifest as increased Ca^{2+} spark size and frequency[12, 21]. Further, in the myocyte Jph2

also interacts with Speg, which can indirectly alter RyR2 and the SR Ca^{2+}-ATPase by phosphorylation and activity[27-29]. While this aberrant Ca^{2+} homeostasis has been linked with the development of cardiomyopathic disease and heart failure, it also serves as an arrhythmic substrate and can generate cellular ectopy and spontaneously depolarizing myocardial cells[10-12]. In this study, we find that Jph2 expression knockdown in the nodal cells causes reduced Ca^{2+} transient amplitude while increasing automaticity of the cell. This is similar to *in vitro* and *in vivo* models of cardiac myocyte models of Jph2 expression silencing[10-12]. Further, our observation that Hcn4:shJph2 isolated nodal cells demonstrate leak of SR store Ca^{2+}, which is driven by increased spark frequency, supports an analogous role for Jph2 in the negative gating regulation of RyR2 seen in cardiac myocytes. Our finding that Ncx1 function is impaired during “resting” membrane potentials is in line with previous work identifying a similar reduction in Jph2 knockdown within cardiac myocytes[21]. This impairment may reflect a regulatory effect of Jph2 on Ncx1. This possibility is supported by evidence that loss of Ncx1 expression in murine nodal cells results in rapid nodal depolarizations and an increase in automaticity[30]. Further, Ca^{2+} leak-driven automaticity is supported by resolution of tachycardic arrhythmias by EL20, a direct RyR2 antagonist. EL20 is a novel tetracaine-derivative that has been shown to diminish arrhythmia burden in a murine model of catecholaminergic polymorphic ventricular tachycardia[20]. While its role on nodal tissue is unexplored, it is believed to reduce the diastolic leak of SR-stored Ca^{2+} by selectively inhibiting RyR2 channels in cardiac myocytes[20]. Given the emerging role of abnormal Ca^{2+} homeostasis and signaling in driving automaticity, our findings suggest that targeting SR-mediated Ca^{2+} leak may be an avenue for the treatment of nodal arrhythmias with increased automaticity.

Calcium clock regulation in nodal cells

The role of SR-mediated Ca^{2+} leak in nodal cell automaticity remains complex. Mutations in *RYR2*, which typically cause increased opening probability of the channel, and resultant leak of SR Ca^{2+}, are a major cause of catecholaminergic polymorphic ventricular tachycardia (CPVT). While the majority of mouse models hosting *RYR2* mutations associated with arrhythmias focus on inducible ventricular arrhythmias in their characterization, there is a small body of work exploring the impact of these mutations on nodal cell automaticity. Interestingly, these mutations are associated with sinus bradycardia and reduced nodal cell automaticity. In one isolated SA nodal cells from the RYR2-R4496C mouse demonstrated reduced Ca^{2+} transient frequency in the setting of increased SR Ca^{2+}leak[31]. The authors also identified reduced L-type Ca^{2+} current leak and reduced SR store Ca^{2+} levels and conclude that it is this reduction in overall Ca^{2+} load the reduces the Ca^{2+} clock control of automaticity. This phenomenon is also present in patients with CPVT for whom *RYR2* mutations result in RYR2-mediated Ca^{2+} leak from the sarcoplasmic reticulum. Rather than sinus tachycardia, which would be expected given the findings from these mice, humans consistently demonstrated sinus bradycardia associated with *RYR2* pathologic mutations[32]. This divergence in phenotype between mouse and human nodal automaticity is also supported by our PheWAS analysis of JPH2, which identified an association between this locus and bradycardic sinus node dysfunction in patients. In at least one genetic model of CPVT, both patients and a knock-in mouse hosting the RYR2-R420Q variant demonstrated bradycardia through impaired Ca^{2+} clock signaling and what

the authors suggest is impaired beta adrenergic modulation of heart rate[33]. This raises the possibility that extracardiac modulators of heart rate, such as increased sympathetic regulation in patients CPVT or in patients with significant bradycardia, may blunt the effect of the intracellular Ca^{2+} clock. This possibility remains largely untested. Finally, while there are clear species-specific differences in nodal cell automaticity response due to inhibition of store Ca^{2+} release, correlative studies to explore variability in humans are largely lacking[34]. Thus, the divergence of these phenotypes remains an open question.

While canonically viewed as a structural protein which plays a role in excitation-contraction coupling and intracellular Ca^{2+} regulation, it has been recently shown that Jph2 plays a critical role in driving the ultrastructural cellular remodeling of cardiac myocytes. Stress-induced calpain-mediated cleavage of Jph2 creates an N-terminal fragment which translocate to the nucleus and initiates a cellular response to this stress[35]. While the transcriptional role of Jph2 in nodal tissue of the heart remains unknown, it is plausible Jph2 may play a role beyond purely direct molecular coupling. It is also possible that other known regulators of the Ca^{2+} clock play still-undefined roles in the observed increased in automaticity; however, future studies are needed to determine this.

Limitations

This study has several limitations. Due to inability to consistently detect atrial depolarizations, we were unable to rigorously determine whether junctional rhythm, or JET, occurred in ambulatory mice using telemeters. It remains unclear whether EL20 blocks any non-RyR2 targets that may play a role in reducing the nodal automaticity observed with Jph2 knockdown. It also remains unclear what the role of the membrane clock is in modulating the automaticity and Ca^{2+} transients observed. Experimentally, measurement of SR Ca^{2+} store in a spontaneously beating nodal cell may be affected by the presence and timing of Ca^{2+} transients at the time of caffeine exposure. The role that NCX current, as well as the kinases PKA and CaMKII, may have in modulating nodal automaticity in this model remains an area of future research. Finally, due to the large number phecodes comprising the PheWAS study, adjustment for multiple comparisons was not performed. Thus, the association between variants in JPH2 and the diseases noted should be considered hypothesis-generating and require further validation to establish a true relationship.

Conclusions

Nodal-specific knockdown of Jph2 expression causes increased nodal automaticity through increased Ca^{2+} leak from intracellular stores. This store Ca^{2+} leak drives faster and more irregular spontaneous nodal depolarizations which increased nodal automaticity and manifest as tachycardia and junctional rhythms in mice. Dysregulated intracellular Ca^{2+} underlies nodal arrhythmogenesis in this mouse model.

Supplementary Material

Refer to Web version on PubMed Central for supplementary material.

Acknowledgments:

We thank Dr. Robert M. Strongin and Dr. Martha Sibrian-Vazquez, Elex Biotech Inc for providing compound EL20.

Sources of Funding:

A.P.L. is supported by the National Institutes of Health (NIH) K08-HL136839, R01-HL149870, Baylor College of Medicine Department of Pediatrics Pilot Grant Award, the Pediatric and Congenital Electrophysiology Society Paul C. Gillette Award, and the Mike Hogg Fund. Q.Y. is supported by Chinese Government Scholarship (University Graduate Program) in Central South University 31801-160170002. R.M.P. is supported by the American Heart Association Predoctoral Fellowship 829638. T.A.W is supported by the NIH grant 1T32 HL139430-01A1. X.H.T.W. is supported by NIH grants R01-HL089598, and R01-HL147108, and R01-HL153350.

Nonstandard Abbreviations and Acronyms

AJR	accelerated junctional rhythm
AP	action potential
APA	action potential amplitude
AV	atrioventricular node
CaMKII	calmodulin-dependent protein kinase II
DDR	diastolic depolarization rate
DI	duration of diastolic depolarization
ECG	electrocardiogram
E_{-th}	action potential threshold potential
EP	electrophysiology
FWHM	full width at half maximum amplitude
FDHM	full duration at half maximum amplitude
GFP	green fluorescent protein
Hcn4	Hcn4-driven cre-recombinase
HR	heart rate
IJ	internal jugular
JET	junctional ectopic tachycardia
JMC	junctional membrane complex
Jph2	junctophilin 2
mTmG	membrane-targeted tdTomato and green fluorescent protein
MDP	maximum diastolic potential
NCX/Ncx1	sodium-calcium exchanger

PKA	protein kinase A
PheWAS	phenome-wide association study
RFP	red fluorescent protein
RyR2	ryanodine receptor type 2
SA	sinoatrial node
ShJph2	Jph2-targeted short-hairpin
SNRT	sinus node recovery time
SR	sarcoplasmic reticulum
V_{-th}	action potential threshold

References:

1. Atkinson AJ, Logantha SJ, Hao G, Yanni J, Fedorenko O, Sinha A, Gilbert SH, Benson AP, Buckley DL, Anderson RH, et al. Functional, anatomical, and molecular investigation of the cardiac conduction system and arrhythmogenic atrioventricular ring tissue in the rat heart. J Am Heart Assoc. 2013;2:e000246. [PubMed: 24356527]
2. Mangoni ME, Nargeot J. Genesis and regulation of the heart automaticity. Physiol Rev. 2008;88:919–82. [PubMed: 18626064]
3. Christoffels VM, Smits GJ, Kispert A and Moorman AF. Development of the pacemaker tissues of the heart. Circ Res. 2010;106:240–54. [PubMed: 20133910]
4. Park DS and Fishman GI. The cardiac conduction system. Circulation. 2011;123:904–15. [PubMed: 21357845]
5. Chiu SN, Wang JK, Wu MH, Chang CW, Chen CA, Lin MT, Wu ET, Hua YC, Lue HC and Taipei Pediatric Cardiology Working G. Cardiac conduction disturbance detected in a pediatric population. J Pediatr. 2008;152:85–9. [PubMed: 18154906]
6. Huser J, Blatter LA and Lipsius SL. Intracellular Ca2+ release contributes to automaticity in cat atrial pacemaker cells. J Physiol. 2000;524 Pt 2:415–22. [PubMed: 10766922]
7. Vinogradova TM, Maltsev VA, Bogdanov KY, Lyashkov AE and Lakatta EG. Rhythmic Ca2+ oscillations drive sinoatrial nodal cell pacemaker function to make the heart tick. Ann N Y Acad Sci. 2005;1047:138–56. [PubMed: 16093492]
8. Wu Y, Valdivia HH, Wehrens XH and Anderson ME. A Single Protein Kinase A or Calmodulin Kinase II Site Does Not Control the Cardiac Pacemaker Ca2+ Clock. Circ Arrhythm Electrophysiol. 2016;9:e003180. [PubMed: 26857906]
9. Landstrom AP, Beavers DL and Wehrens XH. The junctophilin family of proteins: from bench to bedside. Trends Mol Med. 2014;20:353–62. [PubMed: 24636942]
10. Landstrom AP, Kellen CA, Dixit SS, van Oort RJ, Garbino A, Weisleder N, Ma J, Wehrens XH and Ackerman MJ. Junctophilin-2 expression silencing causes cardiocyte hypertrophy and abnormal intracellular calcium-handling. Circ Heart Fail. 2011;4:214–23. [PubMed: 21216834]
11. Landstrom AP, Weisleder N, Batalden KB, Bos JM, Tester DJ, Ommen SR, Wehrens XH, Claycomb WC, Ko JK, Hwang M, et al. Mutations in JPH2-encoded junctophilin-2 associated with hypertrophic cardiomyopathy in humans. J Mol Cell Cardiol. 2007;42:1026–35. [PubMed: 17509612]
12. van Oort RJ, Garbino A, Wang W, Dixit SS, Landstrom AP, Gaur N, De Almeida AC, Skapura DG, Rudy Y, Burns AR, et al. Disrupted junctional membrane complexes and hyperactive ryanodine receptors after acute junctophilin knockdown in mice. Circulation. 2011;123:979–88. [PubMed: 21339484]

13. Beavers DL, Landstrom AP, Chiang DY and Wehrens XH. Emerging roles of junctophilin-2 in the heart and implications for cardiac diseases. Cardiovasc Res. 2014;103:198–205. [PubMed: 24935431]

14. Bolli R. New Initiatives to Improve the Rigor and Reproducibility of Articles Published in Circulation Research. Circ Res. 2017;121:472–479. [PubMed: 28819032]

15. Hoesl E, Stieber J, Herrmann S, Feil S, Tybl E, Hofmann F, Feil R and Ludwig A. Tamoxifen-inducible gene deletion in the cardiac conduction system. J Mol Cell Cardiol. 2008;45:62–9. [PubMed: 18538341]

16. Muzumdar MD, Tasic B, Miyamichi K, Li L and Luo L. A global double-fluorescent Cre reporter mouse. Genesis. 2007;45:593–605. [PubMed: 17868096]

17. Falke LL, Broekhuizen R, Huitema A, Maarseveen E, Nguyen TQ and Goldschmeding R. Tamoxifen for induction of Cre-recombination may confound fibrosis studies in female mice. J Cell Commun Signal. 2017;11:205–211. [PubMed: 28497232]

18. Corrado D, Link MS and Calkins H. Arrhythmogenic Right Ventricular Cardiomyopathy. N Engl J Med. 2017;376:61–72. [PubMed: 28052233]

19. Landstrom AP, Dobrev D and Wehrens XHT. Calcium Signaling and Cardiac Arrhythmias. Circ Res. 2017;120:1969–1993. [PubMed: 28596175]

20. Klipp RC, Li N, Wang Q, Word TA, Sibrian-Vazquez M, Strongin RM, Wehrens XHT and Abramson JJ. EL20, a potent antiarrhythmic compound, selectively inhibits calmodulin-deficient ryanodine receptor type 2. Heart Rhythm. 2018;15:578–586. [PubMed: 29248564]

21. Wang W, Landstrom AP, Wang Q, Munro ML, Beavers D, Ackerman MJ, Soeller C and Wehrens XH. Reduced junctional Na+/Ca2+-exchanger activity contributes to sarcoplasmic reticulum Ca2+ leak in junctophilin-2-deficient mice. Am J Physiol Heart Circ Physiol. 2014;307:H1317–26. [PubMed: 25193470]

22. Rubenstein DS and Lipsius SL. Mechanisms of automaticity in subsidiary pacemakers from cat right atrium. Circ Res. 1989;64:648–57. [PubMed: 2467760]

23. Imtiaz MS, von der Weid PY, Laver DR and van Helden DF. SR Ca2+ store refill--a key factor in cardiac pacemaking. J Mol Cell Cardiol. 2010;49:412–26. [PubMed: 20353793]

24. Vinogradova TM, Lyashkov AE, Zhu W, Ruknudin AM, Sirenko S, Yang D, Deo S, Barlow M, Johnson S, Caffrey JL, et al. High basal protein kinase A-dependent phosphorylation drives rhythmic internal Ca2+ store oscillations and spontaneous beating of cardiac pacemaker cells. Circ Res. 2006;98:505–14. [PubMed: 16424365]

25. Landstrom AP, Beavers DL and Wehrens XHT. The junctophilin family of proteins: from bench to bedside. Trends Mol Med. 2014;20:353–362. [PubMed: 24636942]

26. Reynolds JO, Chiang DY, Wang W, Beavers DL, Dixit SS, Skapura DG, Landstrom AP, Song LS, Ackerman MJ and Wehrens XH. Junctophilin-2 is necessary for T-tubule maturation during mouse heart development. Cardiovasc Res. 2013;100:44–53. [PubMed: 23715556]

27. Quick AP, Wang Q, Philippen LE, Barreto-Torres G, Chiang DY, Beavers D, Wang G, Khalid M, Reynolds JO, Campbell HM, et al. SPEG (Striated Muscle Preferentially Expressed Protein Kinase) Is Essential for Cardiac Function by Regulating Junctional Membrane Complex Activity. Circ Res. 2017;120:110–119. [PubMed: 27729468]

28. Quan C, Li M, Du Q, Chen Q, Wang H, Campbell D, Fang L, Xue B, MacKintosh C, Gao X, et al. SPEG Controls Calcium Reuptake Into the Sarcoplasmic Reticulum Through Regulating SERCA2a by Its Second Kinase-Domain. Circ Res. 2019;124:712–726. [PubMed: 30566039]

29. Campbell HM, Quick AP, Abu-Taha I, Chiang DY, Kramm CF, Word TA, Brandenburg S, Hulsurkar M, Alsina KM, Liu HB, et al. Loss of SPEG Inhibitory Phosphorylation of Ryanodine Receptor Type-2 Promotes Atrial Fibrillation. Circulation. 2020;142:1159–1172. [PubMed: 32683896]

30. Torrente AG, Zhang R, Zaini A, Giani JF, Kang J, Lamp ST, Philipson KD and Goldhaber JI. Burst pacemaker activity of the sinoatrial node in sodium-calcium exchanger knockout mice. Proc Natl Acad Sci U S A. 2015;112:9769–74. [PubMed: 26195795]

31. Neco P, Torrente AG, Mesirca P, Zorio E, Liu N, Priori SG, Napolitano C, Richard S, Benitah JP, Mangoni ME, et al. Paradoxical effect of increased diastolic Ca(2+) release and

decreased sinoatrial node activity in a mouse model of catecholaminergic polymorphic ventricular tachycardia. Circulation. 2012;126:392–401. [PubMed: 22711277]

32. Miyata K, Ohno S, Itoh H and Horie M. Bradycardia Is a Specific Phenotype of Catecholaminergic Polymorphic Ventricular Tachycardia Induced by RYR2 Mutations. Intern Med. 2018;57:1813–1817. [PubMed: 29434162]
33. Wang YY, Mesirca P, Marques-Sule E, Zahradnikova A Jr., Villejoubert O, D'Ocon P, Ruiz C, Domingo D, Zorio E, Mangoni ME, et al. RyR2R420Q catecholaminergic polymorphic ventricular tachycardia mutation induces bradycardia by disturbing the coupled clock pacemaker mechanism. JCI Insight. 2017;2.
34. Lakatta EG, Maltsev VA and Vinogradova TM. A coupled SYSTEM of intracellular Ca2+ clocks and surface membrane voltage clocks controls the timekeeping mechanism of the heart's pacemaker. Circ Res. 2010;106:659–73. [PubMed: 20203315]
35. Guo A, Wang Y, Chen B, Wang Y, Yuan J, Zhang L, Hall D, Wu J, Shi Y, Zhu Q, et al. E-C coupling structural protein junctophilin-2 encodes a stress-adaptive transcription regulator. Science. 2018;362.
36. Bersell K, Choudhury S, Mollova M, Polizzotti BD, Ganapathy B, Walsh S, Wadugu B, Arab S and Kuhn B. Moderate and high amounts of tamoxifen in alphaMHC-MerCreMer mice induce a DNA damage response, leading to heart failure and death. Dis Model Mech. 2013;6:1459–69. [PubMed: 23929941]
37. Sharpe EJ, St Clair JR and Proenza C. Methods for the Isolation, Culture, and Functional Characterization of Sinoatrial Node Myocytes from Adult Mice. J Vis Exp. 2016.
38. Brattelid T, Winer LH, Levy FO, Liestol K, Sejersted OM and Andersson KB. Reference gene alternatives to Gapdh in rodent and human heart failure gene expression studies. BMC Mol Biol. 2010;11:22. [PubMed: 20331858]
39. van Oort RJ, McCauley MD, Dixit SS, Pereira L, Yang Y, Respress JL, Wang Q, De Almeida AC, Skapura DG, Anderson ME, et al. Ryanodine receptor phosphorylation by calcium/calmodulin-dependent protein kinase II promotes life-threatening ventricular arrhythmias in mice with heart failure. Circulation. 2010;122:2669–79. [PubMed: 21098440]
40. Li N and Wehrens XH. Programmed electrical stimulation in mice. J Vis Exp. 2010.
41. Clasen L, Eickholt C, Angendohr S, Jungen C, Shin DI, Donner B, Furnkranz A, Kelm M, Klocker N, Meyer C, et al. A modified approach for programmed electrical stimulation in mice: Inducibility of ventricular arrhythmias. PLoS One. 2018;13:e0201910. [PubMed: 30133474]
42. Adeghe AJ and Cohen J. A better method for terminal bleeding of mice. Lab Anim. 1986;20:70–2. [PubMed: 3951197]
43. Chen B, Wu Y, Mohler PJ, Anderson ME and Song LS. Local control of Ca2+-induced Ca2+ release in mouse sinoatrial node cells. J Mol Cell Cardiol. 2009;47:706–15. [PubMed: 19615376]
44. Verheijck EE, Wessels A, van Ginneken AC, Bourier J, Markman MW, Vermeulen JL, de Bakker JM, Lamers WH, Opthof T and Bouman LN. Distribution of atrial and nodal cells within the rabbit sinoatrial node: models of sinoatrial transition. Circulation. 1998;97:1623–31. [PubMed: 9593568]
45. Schneider CA, Rasband WS and Eliceiri KW. NIH Image to ImageJ: 25 years of image analysis. Nat Methods. 2012;9:671–5. [PubMed: 22930834]
46. Kapoor N, Tran A, Kang J, Zhang R, Philipson KD and Goldhaber JI. Regulation of calcium clock-mediated pacemaking by inositol-1,4,5-trisphosphate receptors in mouse sinoatrial nodal cells. J Physiol. 2015;593:2649–63. [PubMed: 25903031]
47. Picht E, Zima AV, Blatter LA and Bers DM. SparkMaster: automated calcium spark analysis with ImageJ. Am J Physiol Cell Physiol. 2007;293:C1073–81. [PubMed: 17376815]
48. Wang W, Landstrom AP, Wang Q, Munro ML, Beavers D, Ackerman MJ, Soeller C and Wehrens XH. Reduced junctional Na+/Ca2+-exchanger activity contributes to sarcoplasmic reticulum Ca2+ leak in junctophilin-2-deficient mice. Am J Physiol Heart Circ Physiol. 2014;307:H1317–26. [PubMed: 25193470]
49. Mangoni ME and Nargeot J. Properties of the hyperpolarization-activated current (I(f)) in isolated mouse sino-atrial cells. Cardiovasc Res. 2001;52:51–64. [PubMed: 11557233]

50. Roden DM, Pulley JM, Basford MA, Bernard GR, Clayton EW, Balser JR and Masys DR. Development of a large-scale de-identified DNA biobank to enable personalized medicine. Clin Pharmacol Ther. 2008;84:362–9. [PubMed: 18500243]

51. Ruderfer DM, Walsh CG, Aguirre MW, Tanigawa Y, Ribeiro JD, Franklin JC and Rivas MA. Significant shared heritability underlies suicide attempt and clinically predicted probability of attempting suicide. Mol Psychiatry. 2020;25:2422–2430. [PubMed: 30610202]

52. Carroll RJ, Bastarache L and Denny JC. R PheWAS: data analysis and plotting tools for phenome-wide association studies in the R environment. Bioinformatics. 2014;30:2375–6. [PubMed: 24733291]

53. Wei WQ, Teixeira PL, Mo H, Cronin RM, Warner JL and Denny JC. Combining billing codes, clinical notes, and medications from electronic health records provides superior phenotyping performance. J Am Med Inform Assoc. 2016;23:e20–7. [PubMed: 26338219]

54. Dean A, Sullivan K and Soe M. OpenEpi: Open Source Epidemiologic Statistics for Public Health, version 3.01. 2006.

What is Known:

- An intracellular “calcium clock” can regulate the spontaneous automaticity of cardiac nodal cells.

What the Study Adds:

- Reduced Jph2 expression in murine cardiac nodal cells results in increased nodal automaticity and increased leak of calcium from the sarcomplasmic reticulum.
- In vivo expression silencing of Jph2 in mice results in sinus tachycardia and accelerated junctional rhythm, reflecting increased nodal automaticity.
- The *JPH2* gene locus is associated with nodal disease in humans by phenome-wide association.

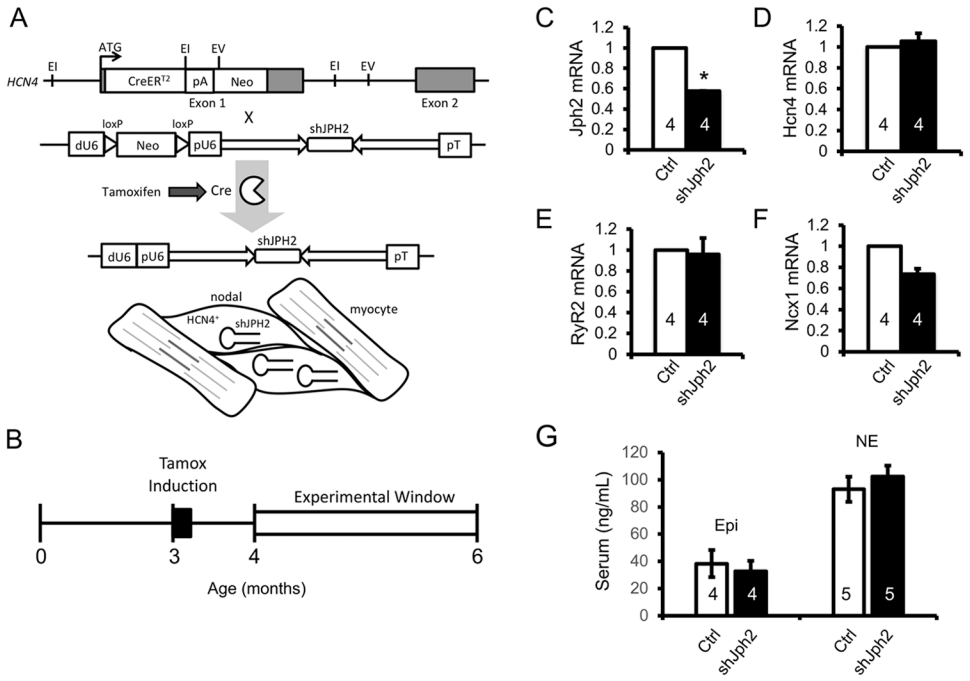

Figure 1:

Experimental mouse Hcn4:shJph2. A) A schematic demonstrating the tamoxifen-inducible Cre-recombinase with expression limited to Hcn4-expressing nodal cells (Hcn4) crossed with an shJph2 expression cassette under a Neo-inhibited promoter (shJph2) to make the experimental line (Hcn4:shJph2). Cre removes an inhibitory neo cassette which allows for loxP excision of the Neo-cassette and fusion of the pU6 promoter to drive expression of an anti-Jph2 short hairpin. B) A schematic of the timeline for induction of Cre by tamoxifen injection and experimental age. C-F) A bar graph demonstrating Jph2, HCN4, RYR2, and NXC1 mRNA expression, respectively, in nodal tissue. G) Plasma ELISA-measured concentration of epinephrine and norepinephrine. * P<0.0001 compared to control.

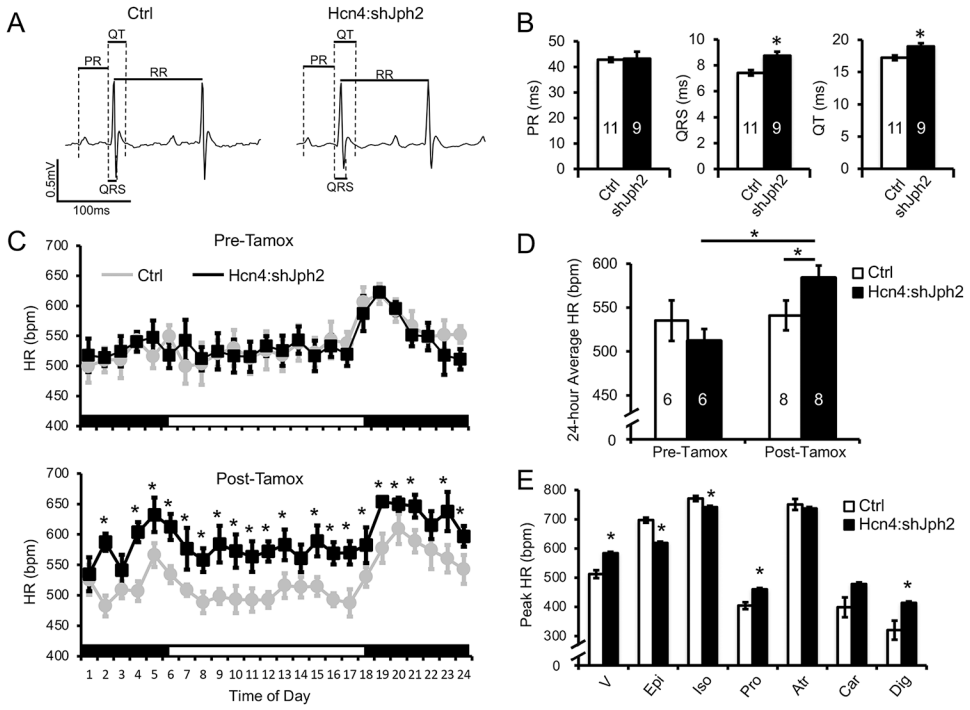

Figure 2:

ECG and telemetry analysis of Hcn4:shJph2 mice. A) Surface ECG and intracardiac EGM show atrial and ventricular depolarization in control and Hcn4:shJph2 mice. B) Bar graphs comparing the PR, QRS, and QT intervals. C and D) Plot and bar graph of telemetry monitored HR over a 24-hour period in control and Hcn4:shJph2 mice pre-tamoxifen (C, top) and post-tamoxifen (C, bottom). E) Bar graph of telemetry monitored change in HR with IP injection of beta-adrenergic agonists (epi, iso), antagonist (pro), muscarinic antagonists (atr) and agonist (car). *P<0.05 compared to control.

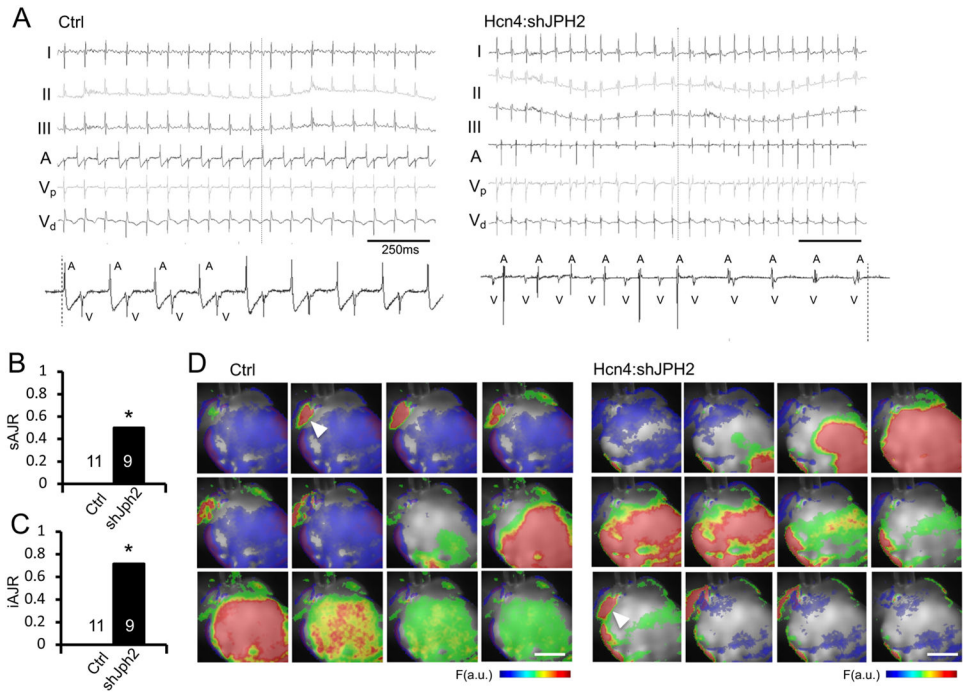

Figure 3:

Intracardiac EP and optical mapping of Hcn4:shJph2 mice. A) Surface ECG (I, II and III) and intracardiac EGMs (atrial, A; proximal ventricle, Vp; distal ventricle, Vd) recordings. Atrial EGM is expanded below with atrial depolarization (A) and ventricular depolarization (V) labeled. Scale bar, 250 ms. B and C) Bar graph of the proportion of spontaneous AJR (B) and adrenergically-induced AJR (C) on intracardiac EP monitoring. D) *Ex vivo* optical mapping demonstrating normal sinus rhythm in the control mice with depolarization (red) starting in the right atria (arrow) and moving from apex to base in the ventricle versus shJph2 mice which demonstrate ventricular depolarization without right atrial depolarization. Scale bar, 2 mm.

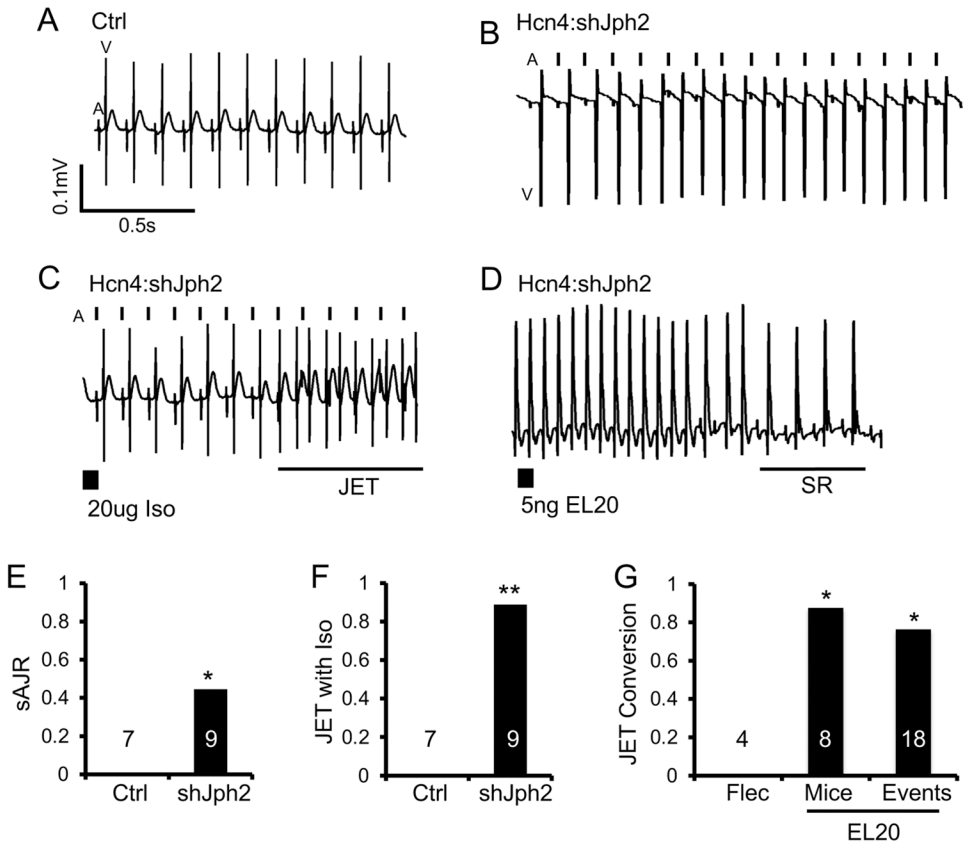

Figure 4:

Epicardial EP monitoring and JET conversion with EL20 application. A and B) *Ex vivo* surface electrode EGM of control and Hcn4:shJph2 mice with atrial depolarization (A and vertical hash lines) and ventricular depolarization (V) labeled. C) Application of beta agonist into the cardiac perfusate (iso) induces rapid onset JET manifest as a narrow complex tachycardia with VA dissociation. D) Application of experimental RyR2 inhibitor EL20 terminates JET to normal sinus rhythm. E and F) Bar graphs demonstrating the proportion of knockdown mice with spontaneous AJR and inducible JET. G) Frequency of conversion of JET with flecainide (flec) and EL20 in each ex vivo heart (mice) and total JET events terminated (events). Vertical lines indicate atrial depolarizations. **P*<0.05, **P<0.001 compared to control

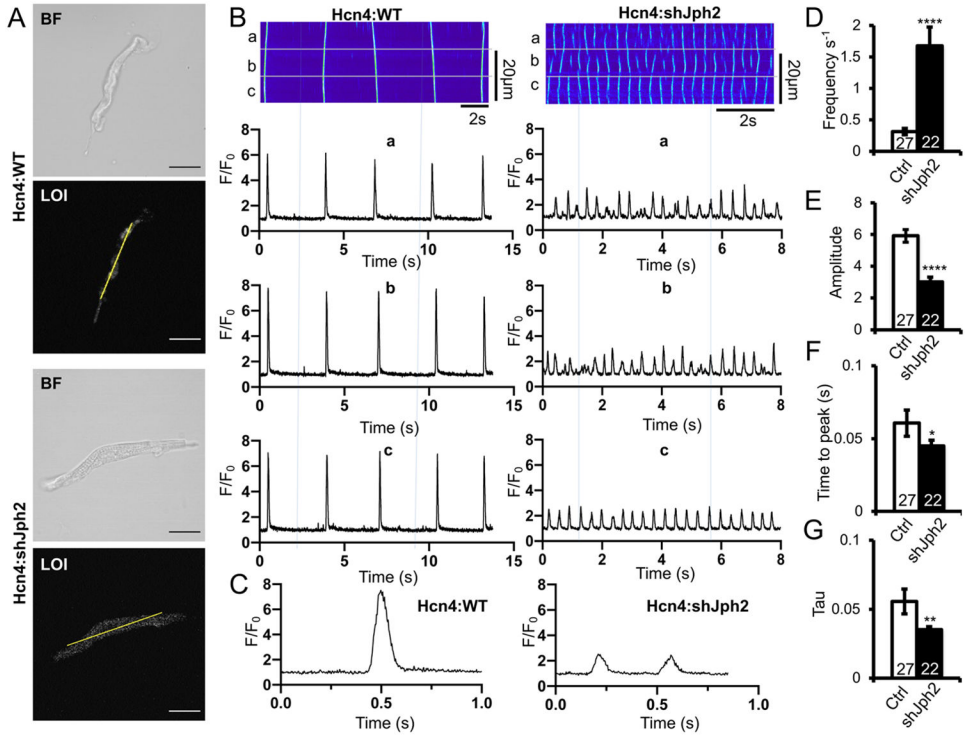

Figure 5:

Jph2 knockdown causes increased nodal cell transient frequency while decreasing transient amplitude. A) Morphology of SA nodal cells in bright field and in LOI field. B) Representative confocal line scan images in Hcn4:WT (left, top) and Hcn4:shJph2 (right, top), and corresponding Ca^{2+} fluorescent tracings (bottom) of observed Ca^{2+} transients at noted positions in line scan images (a, b, and c). C) Representative fluorescence tracings for individual Ca^{2+} transients in Hcn4:WT (left) and Hcn4:shJph2 nodal cells. D-G) Histograms demonstrating the frequency of spontaneous transients (D), transient amplitude (E), transient time-to-peak (F), and time constant of transient decay (tau) (G) in Hcn4:WT mice (white fill) vs. Hcn4:shJph2 mice (black fill). Cell number per analysis is noted in the respective bars. Cells which were derived from 7 Hcn4:WT (Ctrl) and 4 Hcn4:shJph2 mice, respectively. $*P<0.05$, $**P<0.01$, $***P<0.001$, $****P<0.0001$ compared to control.

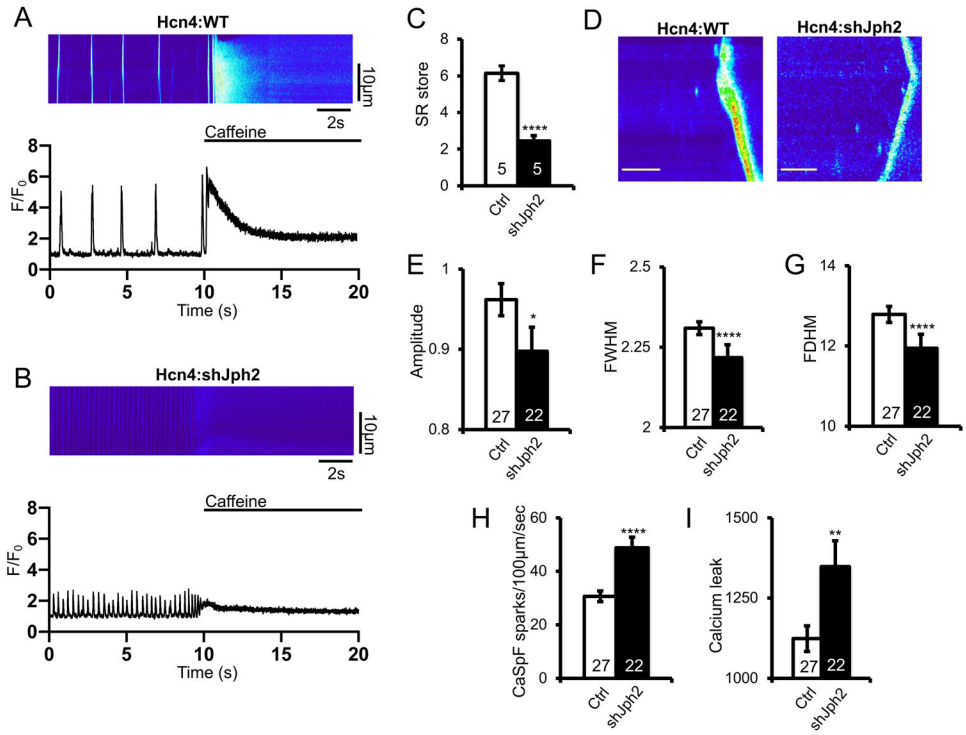

Figure 6:

Jph2 knockdown causes decreased ST-stored Ca^{2+} with increased Ca^{2+} spark frequency and SR Ca^{2+} leak. A-B) Representative line scan images (top) and corresponding Ca^{2+} fluorescent tracings (bottom) of Cal-520 loaded Hcn4:WT (A) and Hcn4:shJph2 (B) nodal cells exposed to caffeine. C) Histogram of store Ca^{2+} release following caffeine exposure. D) Representative line scan images of Ca^{2+} sparks in Hcn4:WT (left) vs. Hcn4:shJph2 (right) mice. E-I) Histograms demonstrating Ca^{2+} spark amplitude (E), width (full width at half maximum amplitude, FWHM) (F), duration (full duration at half-maximum, FDHM (G), CaSpF frequency (H), and calculated Ca^{2+} leak (I) in Hcn4:WT mice (white) vs. Hcn4:shJph2 (black fill) calculated based on the equation $FWHM \times FDHM \times F/F_0 \times CaSpF$. Cell number per analysis is noted in the respective bars. Cells which were derived from 7 Hcn4:WT (Ctrl) and 4 Hcn4:shJph2 mice, respectively. *P<0.05 *P<0.05, **P<0.01, ****P<0.0001.

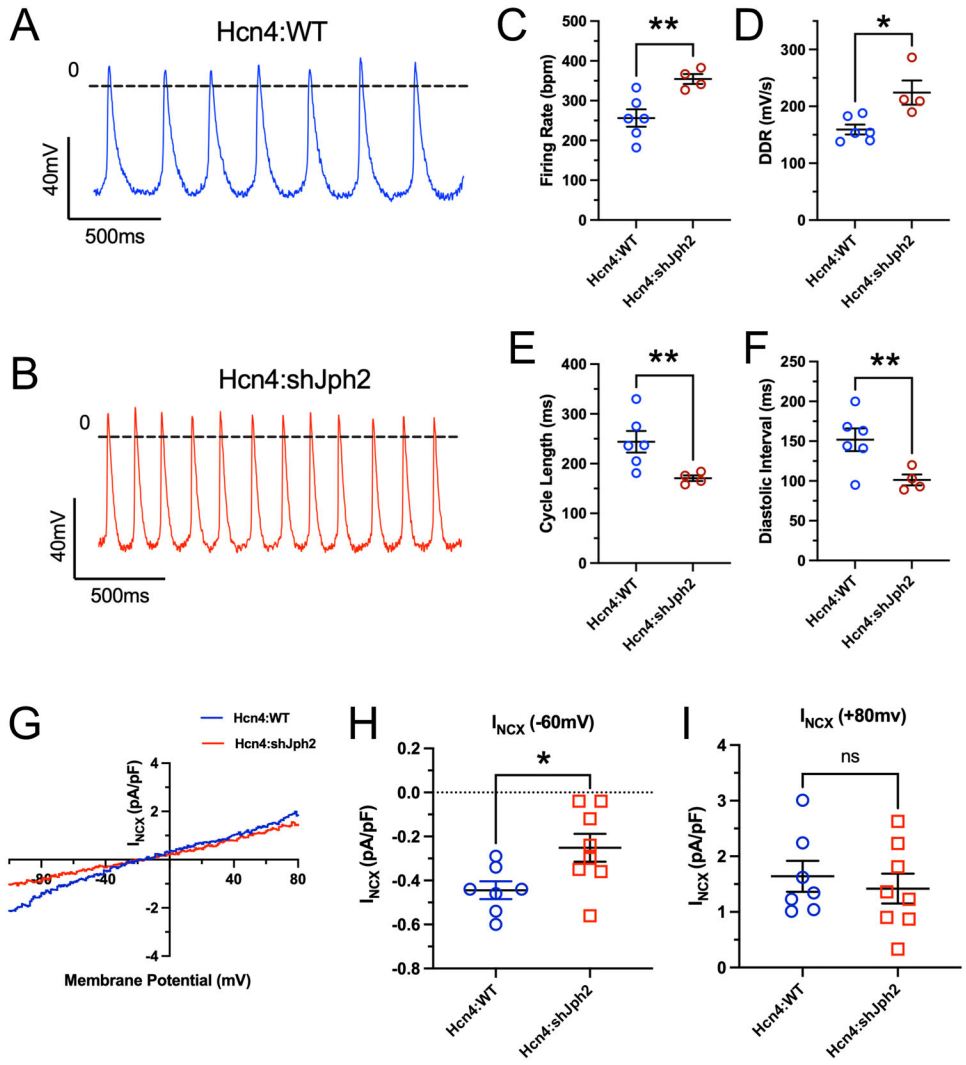

Figure 7:

Jph2 knockdown causes increased cellular automaticity and reduced sodium-calcium exchanger current (I_{NCX}) in SA nodal cells. A and B) Representative action potential recordings of SA nodal cells in Hcn4:shJph2 knock-down mice and Hcn4:WT control mice. C-F) Graphs of the action potential parameters including the AP firing rate (C), diastolic depolarization (DDR, panel D), action potential cycle length (CL, E), and the duration of diastolic depolarization (DI, F). G) Representative traces of I_{NCX} in Hcn4:WT (blue) vs. Hcn4:shJph2 (red) primary SA nodal cells. H and I) Graph of the mean values of I_{NCX} currents of SA nodal cells measured at −60mV (H) and +80mV (I) in Hcn4:WT (blue) vs. Hcn4:shJph2 (red) SA nodal cells. Each cell is identified by an independent data point and were derived from >4 mice. *P<0.05 compared to control. **P<0.01 compared to control. NS, no significant difference.

Table 1:

Top phecodes associated with coding exons in *JPH2*

Phecode	SNP	OR	*P*-value	*N* cases	*N* controls
First degree AV block	rs3810510.42747247.C.T_T	1.50	0.003	228	3775
Atrioventricular block	rs3810510.42747247.C.T_T	1.26	0.004	937	3775
Sinoatrial node dysfunction (bradycardia)	rs3810510.42747247.C.T_T	1.23	0.006	1183	3775
Mobitz II AV block	rs3810510.42747247.C.T_T	2.00	0.006	50	3775

SNP, single nucleotide polymorphism; OR, odds ratio; AV, atrioventricular